ACS chemical biology

Articles

Cite This: ACS Chem. Biol. 2019, 14, 1249−1259

pubs.acs.org/acschemicalbiology

Targeting Dynamic ATP-Binding Site Features Allows Discrimination between Highly Homologous Protein Kinases

Sujata Chakraborty,[†] Takayuki Inukai,[⊥] Linglan Fang,[†] Martin Golkowski,[‡] and Dustin J. Maly*[,†,§]

[†]Department of Chemistry, [‡]Pharmacology, and [§]Biochemistry, University of Washington, Seattle, Washington 98195, United States

[⊥]Medicinal Chemistry Research Laboratories, Ono Pharmaceutical Company, Ltd., 3-1-1 Sakurai, Shimamoto, Mishima, Osaka 618-8585, Japan

Supporting Information

ABSTRACT: ATP-competitive inhibitors that demonstrate exquisite selectivity for specific members of the human kinome have been developed. Despite this success, the identification of highly selective inhibitors is still very challenging, and it is often not possible to rationally engineer selectivity between the ATP-binding sites of kinases, especially among closely related family members. Src-family kinases (SFKs) are a highly homologous family of eight multidomain, nonreceptor tyrosine kinases that play general and specialized roles in numerous cellular processes. The high sequence and functional similarities between SFK members make it hard to rationalize how selectivity can be gained with inhibitors that target the ATP-binding site. Here, we describe the development of a series of inhibitors that are highly selective for the ATP-binding sites of the SFKs Lyn and Hck over other SFKs. By biochemically characterizing how these selective ATP-competitive inhibitors allosterically influence the global conformation of SFKs, we demonstrate that they most likely interact with a binding pocket created by the movement of the conformationally flexible helix αC in the ATP-binding site. With a series of sequence swap experiments, we show that sensitivity to this class of selective inhibitors is due to the identity of residues that control the conformational flexibility of helix αC rather than any specific ATP-binding site interactions. Thus, the ATP-binding sites of highly homologous kinases can be discriminated by targeting heterogeneity within conformationally flexible regions.

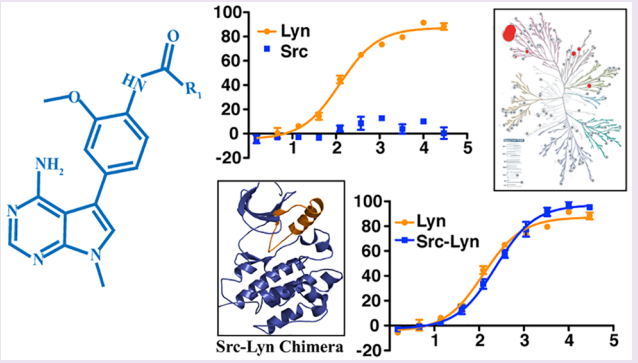

Protein kinases are key regulators of signal transduction pathways and represent a significant portion of the human proteome.[1] All kinases possess a catalytic domain (CD) composed of an N-lobe and a C-lobe with a catalytic cleft that interacts with ATP located between them. Dysregulated kinase activity is associated with a number of human diseases and, for this reason, protein kinase inhibition is an active area of drug discovery.[2,3] There have been significant advancements in our ability to target specific kinases with small molecule inhibitors over the past decade. Despite the fact that a majority of potent and selective small molecule inhibitors target the highly conserved ATP-binding site, it is possible to identify inhibitors that demonstrate exquisite selectivity for a specific kinase target.[4−6] However, the development of highly selective kinase inhibitors is still very challenging, and it is often not possible to rationally engineer discrimination between similar targets because the molecular determinants of specificity are often not well understood. This selectivity problem is particularly acute for closely related subgroups of kinases that possess ATP-binding sites with very few sequence differences.

Most ATP-competitive kinase inhibitors can be classified into three broad categories based on the active site conformation that they stabilize (Figure 1).[7] Many inhibitors, often called type 1, stabilize or are compatible with an "active" ATP-binding site conformation, where all catalytic residues are aligned in an orientation compatible with phosphate transfer. ATP-competitive inhibitors can also stabilize two distinct "inactive" kinase conformations, in which catalytically important residues are displaced from a phosphotransferase-competent orientation. The most common inactive conformation stabilized by ATP-competitive inhibitors is the DFG-out conformation, which is defined by displacement of the Asp-Phe-Gly (DFG)-motif at the base of the activation loop from an active conformation.[8,9] Inhibitors that stabilize the DFG-out conformation, often called type 2, usually possess moieties that make hydrogen bonds with a conserved Glu residue in helix αC and the backbone of the DFG-motif and a large hydrophobic substituent that occupies a pocket created by movement of the Phe residue in the DFG-motif. Potent inhibitors that stabilize an inactive conformation characterized by displacement of helix αC from an active conformation have also been developed.[10−12] Inhibitors that stabilize this inactive form, which is often referred to as the helix

Received: March 17, 2019
Accepted: April 30, 2019
Published: April 30, 2019

DOI: 10.1021/acschembio.9b00214
ACS Chem. Biol. 2019, 14, 1249−1259

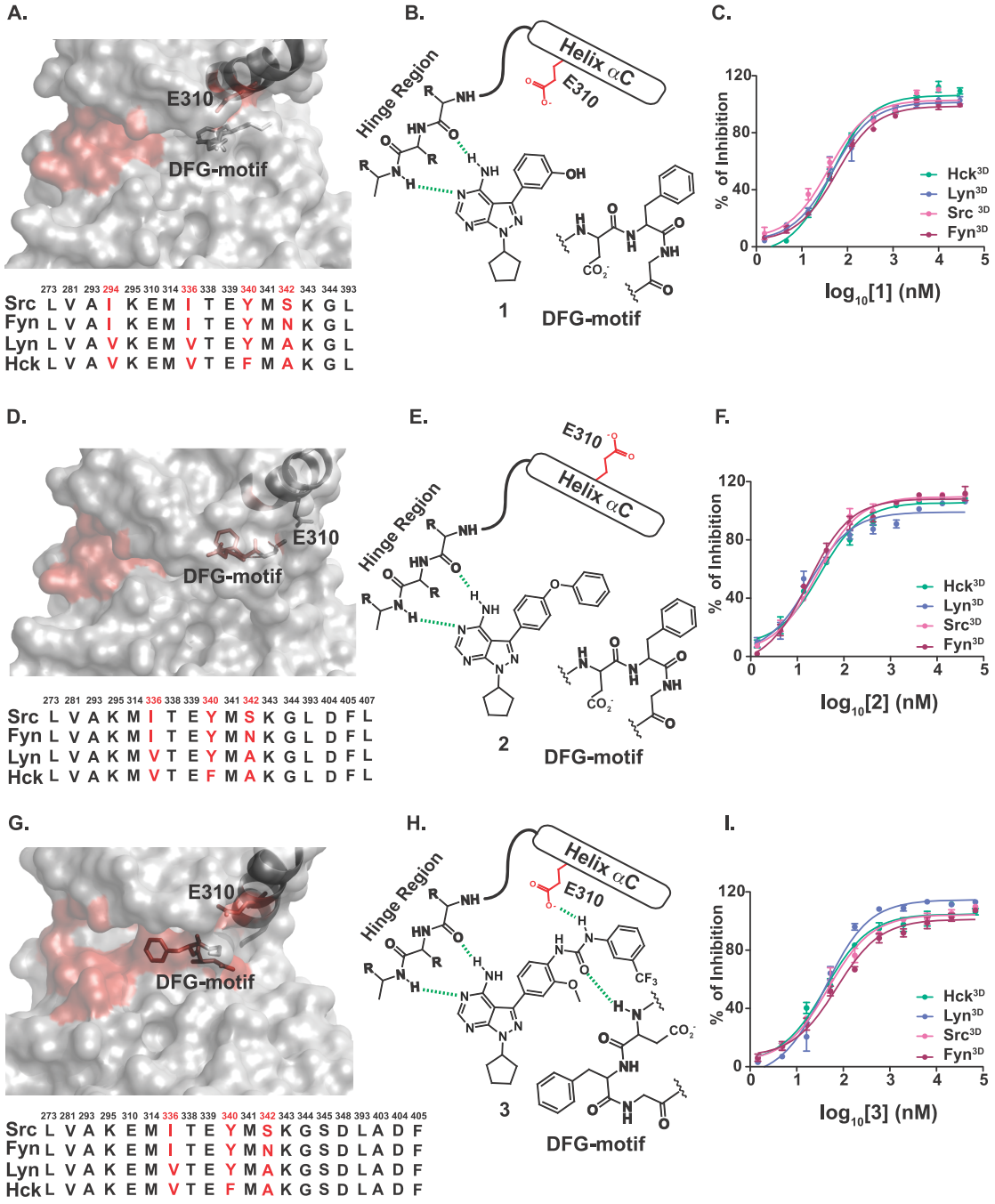

Figure 1. The ATP-binding sites of SFKs are structurally and functionally similar. (A) Cocrystal structure of Src bound to dasatinib (PDB ID, 3G5D; top). Residues that form hydrophobic or polar contacts within 4 Å with dasatinib (identified using Ligplot+)[18] are shown in dark red. Sequence alignment of the 16 hydrophobic or polar dasatinib contact residues for Src, Fyn, Hck, and Lyn (bottom). Residues shown in black are conserved, while residues shown in red vary among these four SFKs. (B) Binding pose of inhibitor **1**, which stabilizes an active ATP-binding site conformation. (C) Inhibitory curves for inhibitor **1** against Src^{3D}, Fyn^{3D}, Hck^{3D}, and Lyn^{3D} activity in the presence of 1 mM ATP ($n = 3$). (D) Crystal structure of Src bound to a helix αC-out-stabilizing analogue of dasatinib (PDB ID, 4YBK; top). Residues that form hydrophobic or polar contacts within 4 Å with helix αC-out-stabilizing dasatinib are shown in dark red. Sequence alignment of the 17 hydrophobic or polar residues that form contacts with helix αC-out-stabilizing dasatinib for Src, Fyn, Hck, and Lyn (bottom). (E) Binding pose of inhibitor **2**, which stabilizes the helix αC-out conformation of the ATP-binding site. (F) Inhibitory curves for inhibitor **2** against Src^{3D}, Fyn^{3D}, Hck^{3D}, and Lyn^{3D} activity in the presence of 1 mM ATP ($n = 3$). (G) Crystal structure of Src bound to a DFG-out-stabilizing analogue of dasatinib (PDB ID, 4YBJ; top). Residues that form hydrophobic or polar contacts within 4 Å with DFG-out-stabilizing dasatinib are shown in dark red. Sequence alignment of the 20 hydrophobic or polar DFG-out-stabilizing dasatinib contact residues for Src, Fyn, Hck, and Lyn (bottom). (H) Binding pose of inhibitor **3**, which stabilizes the DFG-out conformation of the ATP-binding site. (I) Inhibitory curves for inhibitor **3** against Src^{3D}, Fyn^{3D}, Hck^{3D}, and Lyn^{3D} activity in the presence of 1 mM ATP ($n = 3$).

αC-out conformation, usually possess substituents that occupy a pocket created by movement of helix αC. It has been widely speculated that inhibitors that stabilize the DFG-out inactive conformation are inherently more selective than type 1 inhibitors, but recent studies call into question the magnitude of this effect.[8,11] Fewer inhibitors that stabilize the helix αC-out

DOI: 10.1021/acschembio.9b00214
ACS Chem. Biol. 2019, 14, 1249−1259

A.

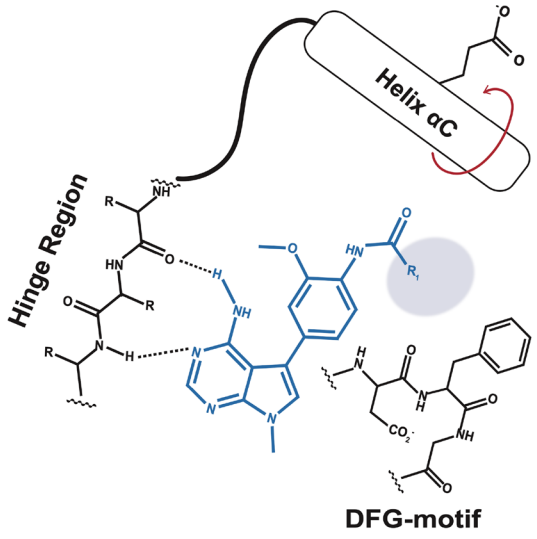

B. K_I (nM) Table

Compound	R_1	Hck^{3D}	Lyn^{3D}	Src^{3D}	Fyn^{3D}	Compound	R_1	Hck^{3D}	Lyn^{3D}	Src^{3D}	Fyn^{3D}
4		< 3.0	< 3.0	6.5 ± 1.5	16 ± 1	13		330 ± 20	40 ± 10	> 2000	> 2000
5	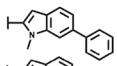	4.7 ± 0.5	< 3.0	180 ± 20	> 2000	14		> 2000	29 ± 8	> 2000	> 2000
6	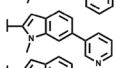	3.9 ± 1.5	< 3.0	130 ± 20	> 2000	15		26 ± 3	3.3 ± 0.4	> 2000	> 2000
7	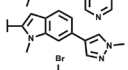	14 ± 2	6.5 ± 1.5	> 2000	> 2000	16	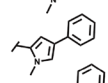	> 2000	61 ± 1	> 2000	> 2000
8		5.4 ± 0.8	< 3.0	110 ± 10	> 2000	17	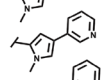	< 3.0	< 3.0	> 2000	> 2000
9	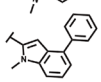	210 ± 10	58 ± 1	> 2000	> 2000	18	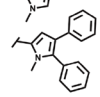	310 ± 20	250 ± 20	> 2000	> 2000
10		> 2000	45 ± 12	> 2000	> 2000	19		3.5 ± 0.6	5.2 ± 0.4	> 2000	> 2000
11	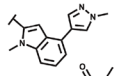	> 2000	8.7 ± 1.1	> 2000	> 2000	20	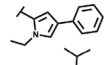	7.2 ± 0.1	4.9 ± 0.7	> 2000	> 2000
12	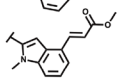	280 ± 10	5.6 ± 1.5	> 2000	> 2000	21		12 ± 1	80 ± 10	50 ± 10	260 ± 20
						22	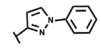	13 ± 2	25 ± 5	> 2000	> 2000

Figure 2. Pyrrolo[2,3-d]pyrimidine-based SFK inhibitors. (A) Structure and proposed ATP-binding mode of the pyrrolopyrimidine-based inhibitors generated and tested. (B) K_I values of inhibitors **4**–**22** against Src^{3D}, Fyn^{3D}, Hck^{3D}, and Lyn^{3D} (mean ± sem, n = 3).

conformation have been characterized, and the inherent selectivity of this ligand class is less understood.

Human Src-family kinases (SFKs) are a family of eight multidomain, nonreceptor tyrosine kinases that play general and specialized roles in numerous cellular processes.[13] SFKs all share regulatory SH2 and SH3 domains that are N-terminal to a highly conserved kinase CD. SFKs are closely related in sequence (64–90% CD sequence identity) and only significantly diverge at their membrane-interacting N-termini and the linker (SH2-kinase domain linker) that connects the SH2 domain to the kinase domain. The SFKs are grouped into two subfamilies, Src-A and Src-B subfamilies (Figure S1A), based on their SH2-kinase domain linker motifs.[14] Despite the importance of SFKs in numerous fundamental processes, there has been limited success in identifying cell-permeable inhibitors that discriminate between family members.[4,15−17] Here, we describe a series of ATP-competitive inhibitors that are highly selective for the Src-B subfamily over the Src-A subfamily SFKs. Using a panel of biochemical assays, we show that these inhibitors promote the autoinhibited form of SFKs, most likely by stabilizing the helix αC-out conformation of the ATP-binding site. Finally, by performing a series of sequence swap experiments, we demonstrate that flexible linker residues that connect helix αC to the N-terminal lobe of the ATP-binding site are responsible for inhibitor sensitivity. Together, these experiments show that it is possible to discriminate between highly similar ATP-binding sites by targeting differences in the conformational flexibility of helix αC.

RESULTS AND DISCUSSION

The kinase domains of SFKs are highly conserved with very few sequence differences in the residues comprising their ATP-

DOI: 10.1021/acschembio.9b00214
ACS Chem. Biol. 2019, 14, 1249−1259

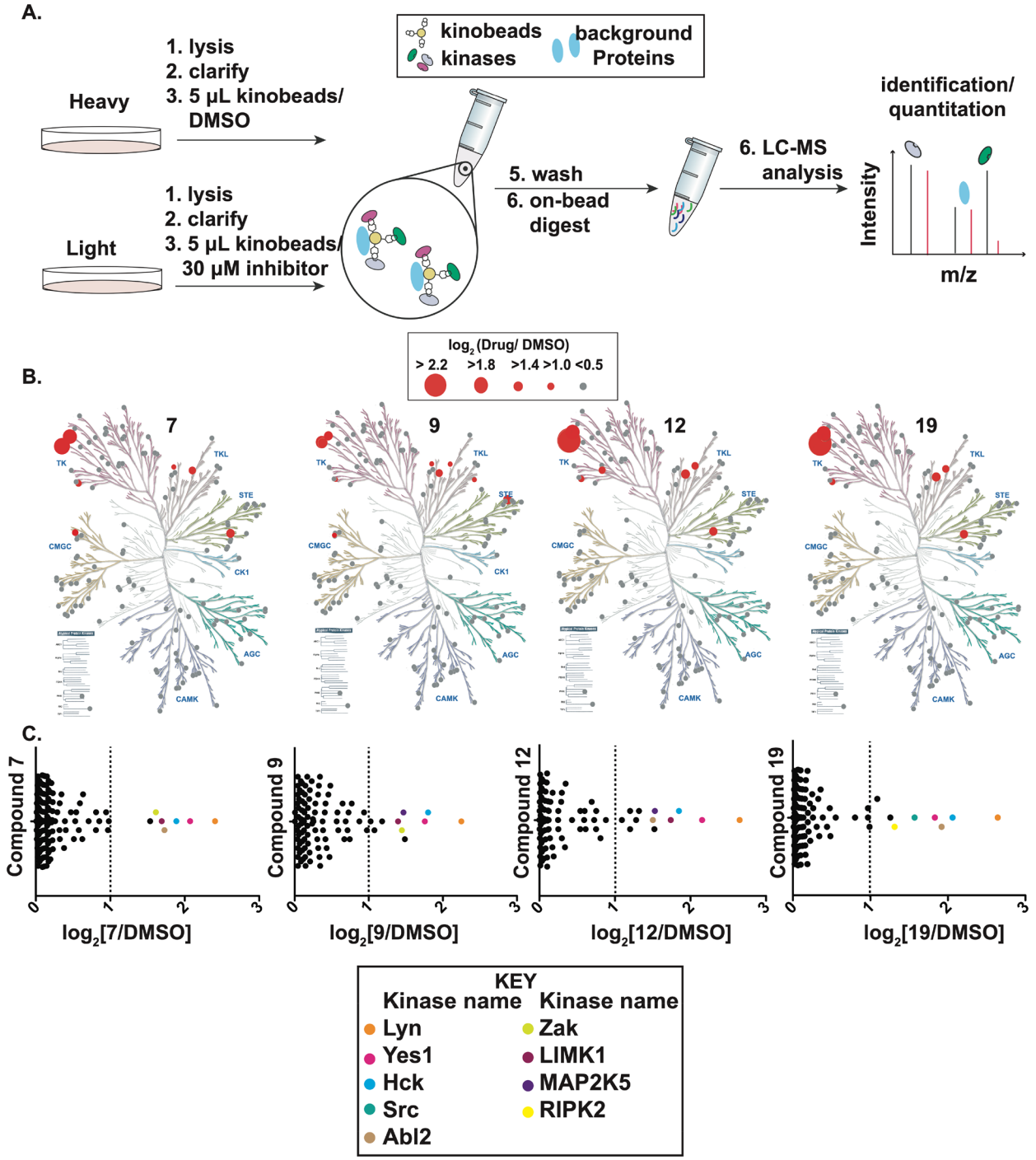

Figure 3. Chemoproteomic profiling of representative inhibitors. (A) Schematic of the kinobead-based profiling method used for profiling inhibitors **7**, **9**, **12**, and **19**.[27] SILAC-labeled HEK293/HCT116 lysates were incubated with DMSO or 30 μM of the inhibitor being profiled and an immobilized matrix of nonselective kinase inhibitors (kinobeads). Captured proteins were subjected to on-bead digestion, identified, and quantified by LC/MS analysis. (B) Phylogenetic trees showing the kinases that were profiled in the chemoproteomic profiling experiments.[28] All profiled kinases are represented by gray circles. Significantly competed kinases are shown as red circles with the size corresponding to the level of competition (larger circle, more competed). Each profiling experiment was performed in duplicate. (C) Transverse waterfall plots of the profiling data shown in part B.

binding sites. To structurally define the similarity of SFK ATP-binding sites, we analyzed cocrystal structures of the CD of Src bound to the drug dasatinib and two conformation-selective analogues of dasatinib (Figure 1A–C).[11] Using these three cocrystal structures, we identified residues that make hydrophobic or polar contacts with each inhibitor (within 4 Å) and performed sequence alignments of inhibitor contact residues for the Group A SFKs Src and Fyn and the Group B SFKs Hck and Lyn (Figure S1B–D). As expected, there are very few sequence differences between Src, Fyn, Hck, and Lyn in the regions that make contact with all three inhibitors (Figure S1B–D). There are 16 residues in Src's ATP-binding site, which is in the active conformation, that make contact with dasatinib. For Src, Fyn, Hck, and Lyn, 12 of these residues are identical, three are similar, and only one, residue 342 (chicken Src numbering), varies substantially (Figures 1A, S1B). Seventeen ATP-binding site

DOI: 10.1021/acschembio.9b00214
ACS Chem. Biol. 2019, 14, 1249–1259

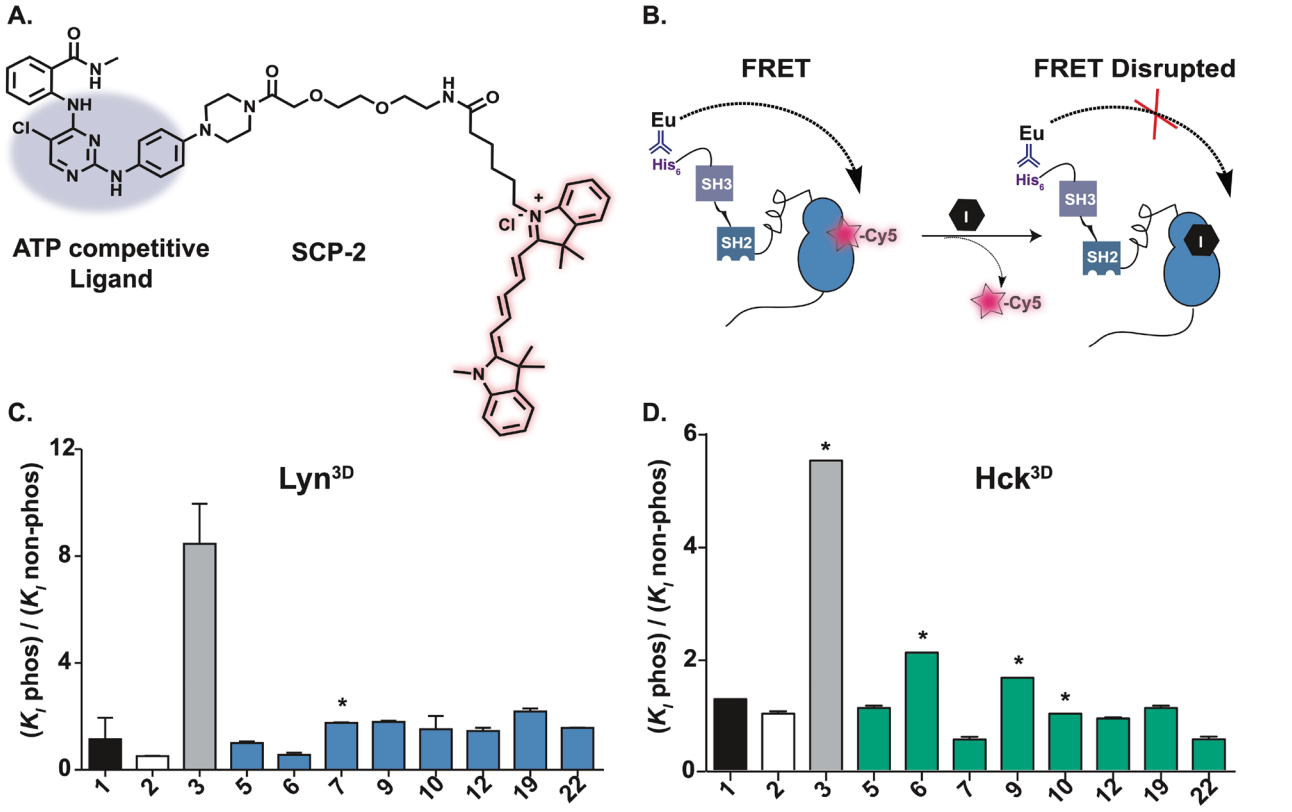

Figure 4. SFK activation loop phosphorylation minimally influences inhibitor potency. (A) Chemical structure of Cy5-labeled probe SCP-2. (B) Schematic of the TR-FRET-based competitive binding assay. A Europium-labeled, anti-His_6 antibody acts as a FRET donor for the Cy5-labeled, ATP-competitive ligand SCP-2. Displacement of SCP-2 with an inhibitor leads to a loss in TR-FRET. (C) Ratio of K_I values determined for phosphorylated and nonphosphorylated Lyn^{3D} ($n = 3$). (D) Ratio of K_I values determined for phosphorylated and nonphosphorylated Hck^{3D} ($n = 3$). K_I values for phosphorylated Lyn^{3D} and Hck^{3D} were determined with an activity assay. K_I values for nonphosphorylated Lyn^{3D} and Hck^{3D} were determined with the competitive binding assay shown in part B. If one or more of the K_I values measured approached the enzyme concentration used in an assay, ratios are denoted with an asterisk (*). K_I values from the TR-FRET-based competitive binding assay are shown in Figure S9B.

residues in Src interact with the helix αC-out version of dasatinib with three residues making unique interactions relative to dasatinib (Figures 1D, S1C). For Src, Fyn, Hck, and Lyn, 14 of these residues are identical, two are similar, and again, only residue 342 varies substantially. Src forms the largest interaction surface with the DFG-out version of dasatinib with 20 ATP-binding site residues making inhibitor contacts (Figures 1G, S1D). However, 17 of these residues are identical and two are similar in Src, Fyn, Hck, and Lyn. Like the other two inhibitors, only contact residue 342 greatly varies between these four kinases (Figure S1D). Residue 342 is located on the hinge region, and its side chain is perpendicular to the ATP-binding site, making it an unlikely source of inhibitor selectivity.

To functionally define the similarities of SFK ATP-binding sites, we tested the sensitivities of Src, Fyn, Hck, and Lyn constructs that contain SH3, SH2, and CDs (SFK^{3D}) to pyrazolopyrimidine-based inhibitors that stabilize either the active (**1**), helix αC-out (**2**), or DFG-out (**3**) conformation of the ATP-binding site (Figures 1B, 1E, 1H). Consistent with the high sequence similarity of their ATP-binding sites, we found that Src^{3D}, Fyn^{3D}, Hck^{3D}, and Lyn^{3D} are equally sensitive to all three inhibitors (Figures 1C, 1F, 1I, S2). Notably, conformation-selective inhibitors **2** and **3** were as nonselective among the SFKs as type 1 inhibitor **1**.

Lyn/Hck-Selective Inhibitors. The sequence and functional similarities between Src, Fyn, Hck, and Lyn makes it hard to rationalize how selectivity can be gained by targeting specific interactions within their ATP-binding sites. However, we observed that differences in the linker connecting the SH2 domain to the CD (SH2-CD linker) of SFKs lead to heterogeneous allosteric coupling between their regulatory and CDs.[19,20] When SFKs are in a closed autoinhibited state, their SH3 domains and SH2-CD linkers form extensive contacts with helix αC in the CD, and these regions are highly coupled through allostery. On the basis of these observations, we predicted that it may be possible to distinguish between the ATP-binding sites of SFKs with inhibitors that make extensive contacts with the region adjacent to helix αC. Therefore, we generated a panel of inhibitors based on a pyrrolo[2,3-*d*]pyrimidine scaffold that should project substituents from its *C*-5 position toward helix αC when forming hydrogen-bonding interactions with the hinge region of SFKs.[21] To provide selectivity for kinases that contain threonine gatekeeper residues, like the SFKs, a 2-methoxyaniline was introduced at the *C*-5 position of the pyrrolo[2,3]pyrimidine scaffold. Acylation of the 2-methoxyaniline allowed us to introduce diverse substituents that we predicted would project toward the helix αCs of SFKs (Figure 2A). Various benzofurans, benzothiophenes, indoles, pyrroles, and pyrazoles were introduced at this position.

We first obtained IC_{50} and K_I values for each inhibitor in our panel against Src^{3D}, Fyn^{3D}, Hck^{3D}, and Lyn^{3D} constructs using a fluorescent reporter activity assay (Figure 2B, S3).[22,23] We observed that while indole **4** potently inhibited all four SFKs, all

DOI: 10.1021/acschembio.9b00214
ACS Chem. Biol. 2019, 14, 1249−1259

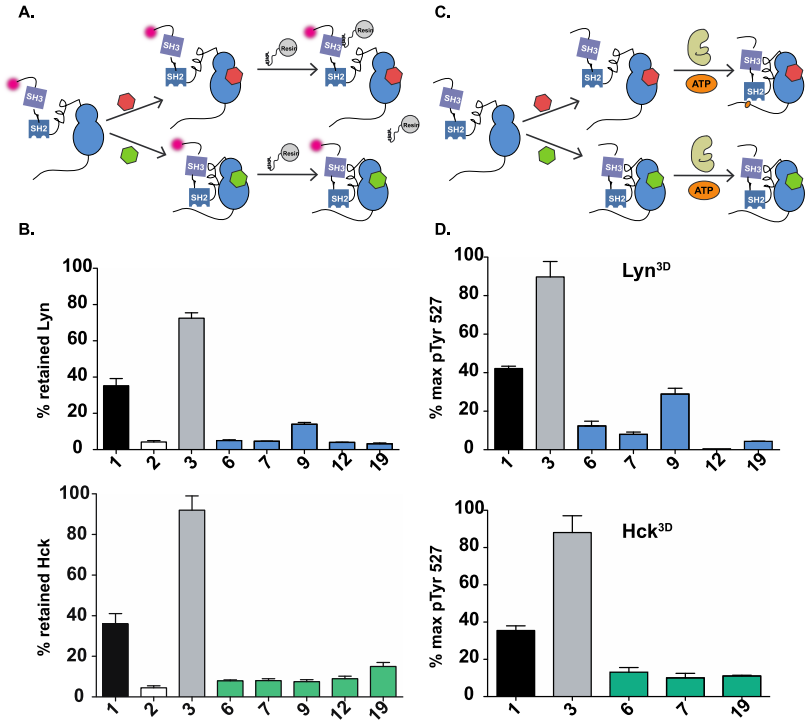

Figure 5. Lyn/Hck-selective inhibitors behave like helix αC-out-stabilizing ligands. (A) Schematic of the SH3 domain ligand pulldown assay using TMR-Lyn^{3D} and TMR-Hck^{3D}. SFK^{3D}-inhibitor complexes are incubated with an immobilized SH3 domain ligand, and the amount of retained kinase is determined after incubation and resin washing. Retained SFKs are quantified after elution using fluorescence imaging. (B) Percent retained Lyn^{3D} (top) and Hck^{3D} (bottom) inhibitor complexes in the SH3 pulldown assay. Values shown are mean ± sem (n = 3). (C) Schematic of the SH2 domain accessibility assay using Csk. SFK^{3D}-inhibitor complexes are incubated with a drug-resistant mutant of Csk (T338I) and γ^{32}P-ATP. Radioactive phosphate transfer to the C-terminal tail of SFKs is quantified. Closed, SH2-engaged Src cannot be phosphorylated by Csk whereas open, SH2-disengaged Src is efficiently phosphorylated by Csk. (D) Quantification of Lyn's (top) and Hck's (bottom) C-terminal phosphorylation by Csk T338I. Values shown are mean ± sem (n = 3).

other derivatives in this series demonstrated high selectivity within the SFKs. Strikingly, all inhibitors are more potent against group B SFKs Hck and Lyn over the group A members Src and Fyn. Notably, **7**, **15**, **17**, **19**, **20**, **22**, and **23** potently inhibited both Hck^{3D} and Lyn^{3D} but had minimal activity against Src^{3D} and Fyn^{3D} at the highest concentration tested (30 μM). Within this group of Hck/Lyn-selective inhibitors, a structural motif consisting of a 5-membered heterocycle with a 1,3-relationship between the aryl group and the amide linkage to the 2-methoxyaniline scaffold is common. Some of the inhibitors in this series were also able to discriminate between Lyn^{3D} and Hck^{3D} with **10**, **11**, and **12** demonstrating at least 40-fold selectivity for Lyn^{3D} over Hck^{3D} with no inhibition of Src^{3D} or Fyn^{3D}. These Lyn-selective inhibitors all contain a 2-carboxyindole with a substituent at the 4-position. Thus, by introducing structural diversity off of the 2-methoxyaniline at the C-5 position, it is possible to discriminate between the highly conserved ATP-binding sites of the SFKs.

Global Profiling of Inhibitor Selectivity. Next, we investigated how the selectivity we observed within the SFKs was reflected throughout the broader kinome. To determine this, we tested four representative inhibitors, **7**, **9**, **12**, and **19**, in a mass spectrometry-based lysate profiling assay (Figure 3A).[24−27] This kinase profiling assay involves determination of the level of competition an inhibitor provides for enriching endogenous kinases in an HCT116/HEK293 cell lysate mixture by an immobilized, nonselective, ATP-competitive inhibitor matrix. We tested each inhibitor at a single high concentration, 30 μM, to identify strong and weak kinase interactors. In total, ~160 kinases were quantitatively profiled in these experiments. We found that **7**, **9**, **12**, and **19** possess fairly narrow specificity profiles and that Lyn was their most competed target (Figure 3B and C, S4). Among the SFKs, Yes and Hck showed the highest level of competition after Lyn. Similar to our *in vitro* inhibition assays with purified constructs, Src and Fyn, as well as closely related FRK, showed significantly lower levels of competition. Furthermore, we observed that our pyrrolopyrimidine-based inhibitors were generally selective for the SFKs with only a handful of non-SFK targets that appeared to be of low to moderate affinity. To obtain an indication of what type of inhibitory potency this low to moderate competition translates to, we performed activity assays with a recombinant construct of Abl1, which was competed at comparable, albeit slightly lower, levels as Abl2/Arg by **9**, **12**, and **19** but did not match our selected cutoff for quantification of significance (Figure S5). We observed that **7**, **9**, **12**, and **19** were at least 60-fold less potent in inhibiting the activity of Abl1 (Figure S6). Thus, our pyrrolopyrimidine-based inhibitors are, in general, selective for Lyn within the SFKs and across the wider kinome.

Influence of Activation Loop Phosphorylation. Next, we determined how activation loop phosphorylation affects the potency and selectivity of our Lyn/Hck-selective inhibitors. We observed that the activation loops of Lyn, Hck, and Src undergo near quantitative phosphorylation on Tyr 416 during the preincubation step in our activity assays (Figure S7). Because activation loop phosphorylation can affect the potencies of some inhibitors for nonreceptor tyrosine kinases,[29,30] we investigated if our inhibitors are sensitive to this modification. To do this, we

DOI: 10.1021/acschembio.9b00214
ACS Chem. Biol. 2019, 14, 1249−1259

developed an assay for ATP-binding site occupancy that does not require measuring kinase activity and can be used with quantitatively dephosphorylated SFKs. Specifically, we used a time-resolved fluorescence resonance energy transfer (TR-FRET)-based competitive binding assay between a Europium-labeled, anti-His_6 antibody bound to the N-termini of SFKs as a FRET donor and a Cy5-labeled, ATP-competitive probe (SCP-2) as a FRET acceptor (Figures 4A and B and S8).[31]

With our TR-FRET assay, we first determined the K_I values of eight (**5**, **6**, **7**, **9**, **10**, **12**, **19**, and **22**) representative inhibitors for dephosphorylated Lyn. Unlike DFG-out-stabilizing inhibitor **3**, all eight inhibitors were nearly equipotent for phosphorylated and dephosphorylated Lyn (Figure 4C, S9). Thus, despite targeting a conformationally flexible region of the SFKs, our Lyn/Hck-selective inhibitors are not sensitive to kinase phosphorylation state. We also tested **5**, **6**, **7**, **9**, **10**, **12**, **19**, and **22** in the TR-FRET assay with Hck and Src. Like Lyn, Hck's and Src's sensitivity to this panel of inhibitors was minimally influenced by their phosphorylation states (Figure 4D, S9). In sum, the phosphorylation state of the SFKs does not appear to have a major effect on their affinities for our panel of Lyn/Hck-selective inhibitors. Furthermore, differences in SFK activation loop phosphorylation in our activity assays cannot account for the dramatic selectivity we observe.

Stabilization of the Helix αC-Out Conformation. We next performed mechanistic studies to further define how Lyn/Hck-selective inhibitors interact with the ATP-binding sites of SFKs. Our pyrrolopyrimidine-based inhibitors were designed to project their *C*-5 substituents into a pocket that is available if helix αC in the N-terminal lobe of the kinase domain moves into an inactive conformation—the helix αC-out inactive conformation. We have previously demonstrated that inhibitors that stabilize the helix αC-out inactive conformation of SFKs allosterically promote a more closed global conformation with enhanced intramolecular SH2 and SH3 domain engagement.[19,20,32,33] In contrast, we have observed that inhibitors that stabilize the DFG-out inactive conformation of the ATP-binding site promote a more open global SFK conformation with SH2 and SH3 domains that are freely accessible to intermolecular binding partners. To test whether our Lyn/Hck-selective inhibitors promote the helix αC-out inactive conformations of Lyn and Hck as designed, a representative panel of SFK-inhibitor complexes was tested in two biochemical assays of SH2 and SH3 domain accessibility.[19,20,23,32,33]

First, we tested the intermolecular accessibility of representative SFK^{3D}-inhibitor complexes in a pulldown assay with an immobilized SH3 domain ligand. To allow quantitative comparisons of the amount of Lyn pulled down in this assay, we generated a Lyn^{3D} construct with a tetramethylrhodamine (TMR) fluorophore at its *N*-terminus using the transpeptidase Sortase A (Figures 5A, S10A).[34] Using the TMR-labeled Lyn construct, we confirmed that inhibitors **1**−**3** lead to expected levels of intermolecular SH3 domain accessibility (Figure 5B, S10B). TMR-Lyn^{3D} bound to helix αC-out-stabilizing inhibitor **2**, which promotes a closed global SFK conformation, demonstrated minimal pulldown in this assay, while TMR-Lyn^{3D} bound to DFG-out-stabilizing inhibitor **3**, which promotes an open global SFK conformation, was efficiently retained by the immobilized SH3 domain ligand. As expected, complexation to inhibitor **1**, which has a minimal influence on the global conformation of SFKs, led to an intermediate level of retained TMR-Lyn^{3D}. With these benchmarks in hand, we next tested the intermolecular accessibility of TMR-Lyn^{3D}'s SH3 domain when complexed to a representative set of pyrrolopyrimidine-based inhibitors. We found that all TMR-Lyn^{3D}-inhibitor complexes exhibited limited pulldown with the immobilized SH3 domain ligand with retained levels comparable to the TMR-Lyn-**2** complex (Figure 5B, S10B). These results strongly suggest that the pyrrolopyrimidine-based inhibitors in our panel promote displacement of Lyn's helix αC from an active conformation, resulting in a closed global conformation with strengthened intramolecular regulatory interactions. We also observed that TMR-Hck^{3D} exhibited limited pulldown (Figure 5B, S10C) when bound to a representative set of pyrrolopyrimidine-based inhibitors, demonstrating that the binding mode of our Lyn/Hck-selective inhibitors is likely conserved among the SFKs.

To probe how inhibitor binding affects intramolecular SFK SH2 domains engagement, we monitored C-terminal tail phosphorylation of SFK^{3D}-inhibitor complexes by C-terminal Src kinase (Csk).[35−38] We previously demonstrated that the amount of C-terminal tail phosphorylation by Csk is highly sensitive to the global conformation of SFK^{3D} constructs. Open, regulatory domain-disengaged SFKs are efficient Csk substrates, while closed, regulatory domain-engaged SFKs exhibit limited phosphorylation by Csk (Figure 5C, 5D).[19,20] Prior to testing inhibitors in the C-terminal tail phosphorylation assay, we first determined whether the required concentrations (3−5 μM) used to form near quantitative SFK-inhibitor complexes directly inhibit the activity of the Csk construct used in this assay. To do this, we monitored Csk's ability to phosphorylate a Lyn construct, Lyn^{CD}, that consists of only the catalytic domain (CD) and C-terminal tail. Because Lyn^{CD} does not contain an SH2 domain capable of shielding the C-terminal tail from phosphorylation, any diminution observed must be due to direct inhibition of Csk. Because our prototypical helix αC-out-stabilizing inhibitor **2** reduced the ability of Csk to phosphorylate Lyn^{CD}, it could not be used as a benchmark for C-terminal tail phosphorylation levels when Lyn is in the closed global conformation. However, inhibitors **1** and **3** displayed no such liability. Consistent with their high kinome selectivity, all representative pyrrolopyrimidine-based inhibitors tested minimally affected Csk's ability to phosphorylate Lyn^{CD} (Figure S11A). Similar to our observations with other SFKs, Lyn^{3D} was a more efficient substrate for Csk when complexed to DFG-out-stabilizing inhibitor **3**, which promotes an open global conformation, than when bound to **1**.[19] All representative pyrrolopyrimidine-based inhibitor-Lyn^{3D} complexes tested displayed lower levels of C-terminal tail phosphorylation than the **1**-Lyn^{3D} complex, which further suggests that they stabilize the helix αC-out ATP-binding site conformation and promote a closed, autoinhibited global conformation. We also observed that representative pyrrolopyrimidine-based inhibitors similarly influenced Csk's ability to phosphorylate the C-terminal tail of Hck^{3D} (Figure 5D, S11B). Together, these biochemical studies suggest that our pyrrolopyrimidine-based inhibitors stabilize the helix αC-out conformation of SFKs and that contacts within this region most likely are responsible for inhibitor potency and selectivity.

Sequence Determinants of Inhibitor Sensitivity. The mechanistic studies above suggest that our pyrrolopyrimidine-based inhibitors stabilize the helix αC-out conformation and likely require large movements within this region of the ATP-binding site. This suggests that their selectivity within the SFKs is most likely due to sequence differences within helix αC or in residues that influence the conformation of this region of the

DOI: 10.1021/acschembio.9b00214
ACS Chem. Biol. 2019, 14, 1249−1259

A.

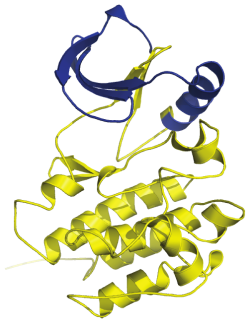

LynS^{CD1}
Residue 244 - 314: Src
Residue 314 - 533: Lyn

C.

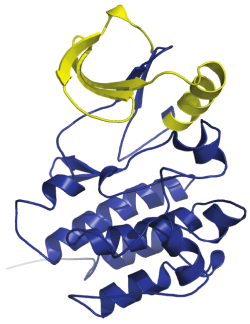

SrcL^{CD1}
Residue 315 - 533: Src
Residue 244 - 314: Lyn

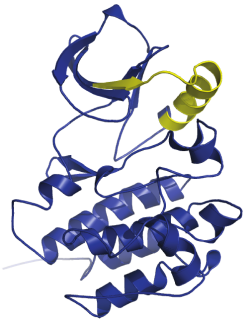

SrcL^{CD2}
Residue 244 - 293; 315 - 533: Src
Residue 294 - 314: Lyn

B.

Compound	K_I (nM) Lyn^{CD}	Src^{CD}	LynS^{CD1}
5	< 3.0	> 2000	49 ± 9
6	2.3 ± 0.1	> 2000	> 2000
7	4.6 ± 0.8	> 2000	> 2000
9	41 ± 9	> 2000	> 2000
10	33 ± 5	> 2000	> 2000
12	4.3 ± 0.5	> 2000	> 2000
19	2.5 ± 0.1	> 2000	> 2000
22	51 ± 7	> 2000	> 2000

D.

Compound	K_I (nM) SrcL^{CD1}	SrcL^{CD2}
5	85 ± 5	78 ± 11
6	89 ± 11	66 ± 6
7	140 ± 30	152 ± 45
9	> 2000	> 2000
10	> 2000	> 2000
12	310 ± 80	> 2000
19	98 ± 8	150 ± 20
22	> 2000	> 2000

Figure 6. Inhibitor sensitivity of Lyn-Src chimeras. (A) Crystal structure of the SH1 domain (Src^{CD}) from PDB ID, 2SRC (Note: only the SH1 domain (CD) from 2SRC, which contains the SH3, SH2, and SH1 domains, is shown for all crystal structures in Figures 6 and 7 because all K_I values shown were determined against constructs that lack SH2 and SH3 domains). The regions of Lyn (yellow) that were swapped with regions from Src (blue) in chimera LynS^{CD1} are shown. (B) K_I values of a representative panel of Lyn/Hck-selective inhibitors for Lyn^{CD}, Src^{CD}, and LynS^{CD1} (values shown are mean ± sem (n = 3)). (C) Crystal structures of Src^{CD} showing the regions of Src (blue) that were swapped with regions from Lyn (yellow) in chimeras SrcL^{CD1} (left) and SrcL^{CD2} (right). (D) K_I values of a representative panel of Lyn/Hck-selective inhibitors for SrcL^{CD1} and SrcL^{CD2} (values shown are mean ± sem (n = 3)).

ATP-binding site. To determine if we could identify these sequence differences, we generated a series of chimeric constructs consisting of an inhibitor-sensitive SFK−Lyn and inhibitor-resistant SFK−Src (Figure 6A). Until this point, all inhibition and biochemical assays, except Figure S11, were performed with SFK constructs that possess an SH3, SH2, and CD (SFK^{3D} constructs). To limit sample search space and allow more facile protein expression and purification, we first determined whether the regulatory domains of Src or Lyn influence their sensitivities to pyrrolopyrimidine-based inhibitors. We found that Src and Lyn constructs containing only the catalytic domain (Src^{CD} and Lyn^{CD}) were similarly inhibited by a representative set of inhibitors as SFK^{3D} constructs, although **5** and **6** were less potent against Src^{CD} than Src^{3D} (Figures 2B, 6B). Therefore, we generated and tested chimeras that only contain CDs and lack SH2 and SH3 domains. First, we generated a Lyn chimera (LynS^{CD1}) that consists of a majority of Src's N-terminal lobe by swapping residues 258−315 between the two SFKs (Figure 6A, S12). Consistent with the N-terminal lobe serving as a key region of pyrrolopyrimidine-based inhibitor sensitivity, we found that LynS^{CD1} was almost completely insensitive to a representative set of inhibitors (Figure 6B).

Having established that Src's N-terminal lobe is sufficient to provide resistance to our pyrrolopyrimidine-based inhibitors, we next determined whether we could sensitize Src through the introduction of residues from Lyn's N-terminal lobe. To do this, we generated two Src chimeras, SrcL^{CD1} and SrcL^{CD2}, that possess different regions of Lyn's N-terminal lobe (Figure 6C). The Src chimera SrcL^{CD1}, which contains residues 258−314 from Lyn, displayed increased sensitivity to several inhibitors: **5**, **6**, **7**, **12**, and **19** (Figure 6D). Furthermore, a Src chimera, SrcL^{CD2}, containing a smaller region of Lyn's N-terminal lobe (residues 294−314) displayed a level of inhibitor sensitivity similar to that of SrcL^{CD1} (Figure 6E). As both SrcL^{CD1} and SrcL^{CD2} contain most of helix αC from Lyn, we narrowed our focus on this region of the ATP-binding site.

Next, we generated a Src chimera, SrcL^{CD3}, that contains the entire helix αC of Lyn and the linker residues that connect it to the β3 and β4 strands of the N-terminal lobe by swapping residues 304−324 between these two SFKs (Figure 7A, S12). Remarkably, introducing this ∼20 residue region of Lyn into Src provided high sensitivity to all of the inhibitors in our representative panel (Figure 7B). There are nine residues that differ between Src and Lyn in the region that spans residues 304−324. Four of these differing residues (305, 309, 312, and 313) are in the structured region of helix αC, and five are in the residues that connect helix αC to the N-terminal lobe. To probe whether residues within helix αC or the linkers that connect this

DOI: 10.1021/acschembio.9b00214
ACS Chem. Biol. 2019, 14, 1249−1259

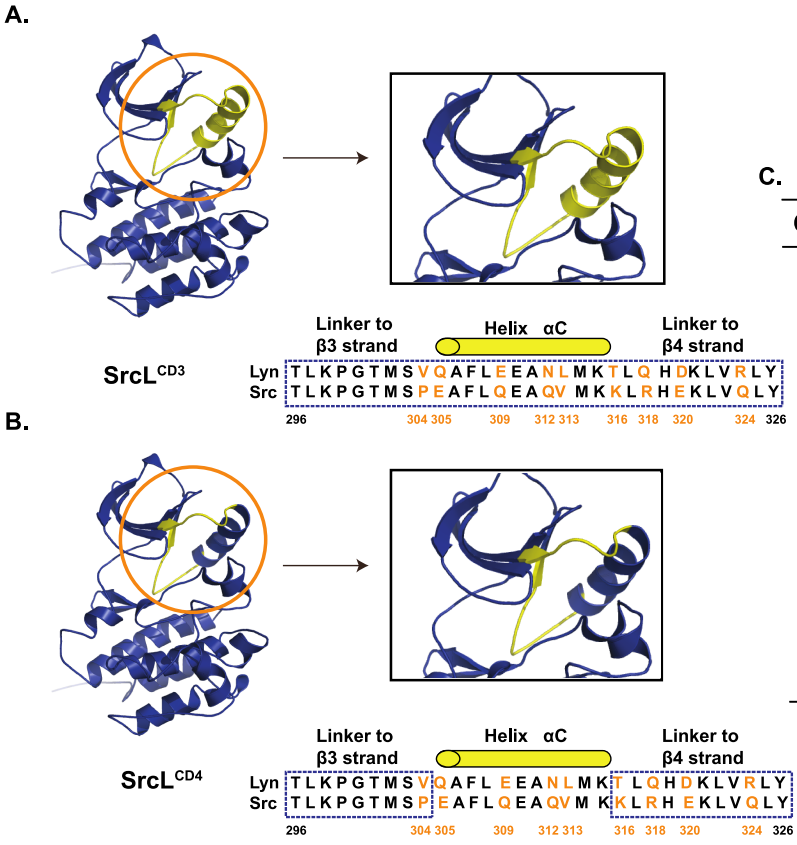

C.

Compound	K_I (nM) SrcL^{CD-3}	SrcL^{CD-4}
5	11 ± 2	16 ± 4.6
6	13 ± 3	15 ± 2
7	21 ± 1	44 ± 8
9	98 ± 14	310 ± 10
10	85 ± 12	450 ± 20
12	18 ± 3	22 ± 3
19	29 ± 7	45 ± 7
22	57 ± 9	37 ± 9

Figure 7. Inhibitor-sensitive Src chimeras containing Lyn's helix αC. (A, B) Crystal structures of the SH1 domain of Src (Src^{CD}) (PDB ID, 2SRC) showing the regions of Src (blue) that were swapped with regions from Lyn (yellow) in chimeras SrcL^{CD3} and SrcL^{CD4}. Insets show an enlarged version of the area circled in the left panel. A sequence alignment of Lyn and Src showing the residues that have been swapped (boxed) in Src is shown below each inset. Residues that differ between Lyn and Src are colored orange. (C) K_I values of a representative panel of Lyn/Hck-selective inhibitors for LynS^{CD3} and LynS^{CD4} (values shown are mean ± sem (n = 3)).

structured region to the N-terminal lobe are responsible for inhibitor sensitivity, we generated the Src chimera SrcL^{CD4} (Figure 7C). SrcL^{CD4} contains the entire C- and N-lobes of Src, including the helical region of helix αC, except for the five sequence differences in the residues that connect helix αC to the N-terminal lobe from Lyn. Consistent with the conformational preference of Lyn's helix αC being responsible for its high sensitivity to Lyn/Hck-selective inhibitors, SrcL^{CD4} is almost equally sensitive to our representative panel of Lyn/Hck-selective inhibitors as SrcL^{CD3} (Figure 7D). Thus, the conformational flexibility of Lyn's helix αC, which is controlled by N-lobe connecting residues, appears to be responsible for its sensitivity to Lyn/Hck-selective inhibitors rather than the presence or absence of specific interactions. For inhibitors like **9** and **10**, which are several-fold more potent against SrcL^{CD3} than SrcL^{CD4}, Lyn's sensitivity may stem from both the conformational preference of helix αC and specific contacts with helix αC itself. Together, our data show that high selectivity among the SFKs can be achieved by targeting the conformational preference of helix αC.

CONCLUSIONS

Diverse strategies are needed for identifying inhibitors that are capable of discriminating between the ATP-binding sites of kinases that possess high sequence homology, like the SFKs. Here, we show that, unsurprisingly, the ATP-binding sites of SFKs are equally susceptible to different modes of ATP-competitive inhibition. However, by modifying a nonselective scaffold with substituents that project toward the conformationally flexible helix αC, we were able to generate ATP-competitive inhibitors that are highly selective for group B SFKs Hck and/or Lyn over Group A members Src and Fyn. Biochemical analyses of how these inhibitors allosterically modulate SFK regulatory domain engagement confirm that they displace helix αC from an active conformation. Our Lyn/Hck-selective inhibitors, in general, possess substituents that would be expected to require large movements of helix αC to be accommodated in SFK ATP-binding sites. Whether the helix αCs of Hck and Lyn are capable of larger movements or pay a smaller energetic penalty for adopting an inactive conformation than Src and Fyn remains to be determined. The ability to identify inhibitors that discriminate between SFKs is somewhat reminiscent of the mechanism proposed for how the ATP-competitive inhibitor FRAX597 is able to selectivity inhibit Group II p21-activated kinases (PAKs) over Group I PAKs.[39] While FRAX597 does not displace helix αC from an active position in PAKs, the apparent increased conformational flexibility of a residue on Group II PAKs' helix αC allows more favorable accommodation of FRAX597 despite Group I PAKs containing identical contact residues in this region. Therefore, it is also a possibility that the helix αC of Lyn and Hck is no more mobile than that of Src and Fyn but that residues in this region can adopt unique rotamer configurations when these SFKs are in the helix αC-out conformation. Regardless of the exact mechanism of discrimination, out sequence swap experi-

DOI: 10.1021/acschembio.9b00214
ACS Chem. Biol. 2019, 14, 1249−1259

ments strongly implicate the flexible linker residues connected to helix αC as being responsible for inhibitor sensitivity.

■ ASSOCIATED CONTENT

Supporting Information

The Supporting Information is available free of charge on the ACS Publications website at DOI: 10.1021/acschembio.9b00214.

Supplementary Excel File 1, containing the MaxQuant output data for inhibitor profiling from HEK293/HCT116 cell lysate (XLSX)

Supplemental Figures S1−12, methods, protein amino acid sequences and DNA sequences, synthetic procedures, and inhibitor characterization (PDF)

■ AUTHOR INFORMATION

Corresponding Author

*E-mail: djmaly@uw.edu.

ORCID

Martin Golkowski: 0000-0002-0996-1655

Dustin J. Maly: 0000-0003-0094-0177

Notes

The authors declare no competing financial interest.

■ ACKNOWLEDGMENTS

This work was supported by the National Institutes of Health (Grants R01GM086858 (D.J.M.) and R01DK116064 (D.J.M.)), Ono Pharmaceutical Co, and a National Science Foundation GRFP (E.M.D.).

■ ABBREVIATIONS

SFKs, Src family kinases; CD, catalytic domain (SH1 domain of kinase); 3D, three domain SFK containing CD (SH1), SH2 and SH3 domains; EDTA, ethylenediaminetetraacetic acid; HEPES, *N*-(2-hydroxyethyl)piperazine-*N*′-2-ethanesulfonic acid; DTT, dithiothreitol; BSA, bovine serum albumin; EGTA, ethylene glycol bis(2-aminoethyl ether)-*N*,*N*,*N*′,*N*′- tetraacetic acid; PMSF, phenylmethylsulfonyl fluoride; IPTG, isopropyl β-D-1-thiogalactopyranoside; Cy5, cyanine 5; TMR, 6-carboxytetramethylrhodamine; Ni-NTA, Ni^{2+}-nitrilotriacetate; BME, β-mercaptoethanol; Tris, tris(hydroxymethyl)aminomethane; DMSO, dimethyl sulfoxide; NMR, nuclear magnetic resonance; MS, mass spectrometry

■ REFERENCES

(1) Manning, G., Whyte, D. B., Martinez, R., Hunter, T., and Sudarsanam, S. (2002) The protein kinase complement of the human genome. *Science 298*, 1912−1934.

(2) Lahiry, P., Torkamani, A., Schork, N. J., and Hegele, R. A. (2010) Kinase mutations in human disease: interpreting genotype-phenotype relationships. *Nat. Rev. Genet. 11*, 60−74.

(3) Ferguson, F. M., and Gray, N. S. (2018) Kinase inhibitors: the road ahead. *Nat. Rev. Drug Discovery 17*, 353−377.

(4) Brandvold, K. R., Steffey, M. E., Fox, C. C., and Soellner, M. B. (2012) Development of a highly selective c-Src kinase inhibitor. *ACS Chem. Biol. 7*, 1393−1398.

(5) Telliez, J. B., Dowty, M. E., Wang, L., Jussif, J., Lin, T., Li, L., Moy, E., Balbo, P., Li, W., Zhao, Y., Crouse, K., Dickinson, C., Symanowicz, P., Hegen, M., Banker, M. E., Vincent, F., Unwalla, R., Liang, S., Gilbert, A. M., Brown, M. F., Hayward, M., Montgomery, J., Yang, X., Bauman, J., Trujillo, J. I., Casimiro-Garcia, A., Vajdos, F. F., Leung, L., Geoghegan, K. F., Quazi, A., Xuan, D., Jones, L., Hett, E., Wright, K., Clark, J. D., and Thorarensen, A. (2016) Discovery of a JAK3-Selective Inhibitor: Functional Differentiation of JAK3-Selective Inhibition over pan-JAK or JAK1-Selective Inhibition. *ACS Chem. Biol. 11*, 3442−3451.

(6) Xia, W., Mullin, R. J., Keith, B. R., Liu, L. H., Ma, H., Rusnak, D. W., Owens, G., Alligood, K. J., and Spector, N. L. (2002) Anti-tumor activity of GW572016: a dual tyrosine kinase inhibitor blocks EGF activation of EGFR/erbB2 and downstream Erk1/2 and AKT pathways. *Oncogene 21*, 6255−6263.

(7) Roskoski, R., Jr. (2016) Classification of small molecule protein kinase inhibitors based upon the structures of their drug-enzyme complexes. *Pharmacol. Res. 103*, 26−48.

(8) Zhao, Z., Wu, H., Wang, L., Liu, Y., Knapp, S., Liu, Q., and Gray, N. S. (2014) Exploration of type II binding mode: A privileged approach for kinase inhibitor focused drug discovery? *ACS Chem. Biol. 9*, 1230−1241.

(9) Liu, Y., and Gray, N. S. (2006) Rational design of inhibitors that bind to inactive kinase conformations. *Nat. Chem. Biol. 2*, 358−364.

(10) Georghiou, G., Kleiner, R. E., Pulkoski-Gross, M., Liu, D. R., and Seeliger, M. A. (2012) Highly specific, bisubstrate-competitive Src inhibitors from DNA-templated macrocycles. *Nat. Chem. Biol. 8*, 366−374.

(11) Kwarcinski, F. E., Brandvold, K. R., Phadke, S., Beleh, O. M., Johnson, T. K., Meagher, J. L., Seeliger, M. A., Stuckey, J. A., and Soellner, M. B. (2016) Conformation-Selective Analogues of Dasatinib Reveal Insight into Kinase Inhibitor Binding and Selectivity. *ACS Chem. Biol. 11*, 1296−1304.

(12) Palmieri, L., and Rastelli, G. (2013) Alpha C helix displacement as a general approach for allosteric modulation of protein kinases. *Drug Discovery Today 18*, 407−414.

(13) Ingley, E. (2008) Src family kinases: regulation of their activities, levels and identification of new pathways. *Biochim. Biophys. Acta, Proteins Proteomics 1784*, 56−65.

(14) Williams, J. C., Wierenga, R. K., and Saraste, M. (1998) Insights into Src kinase functions: structural comparisons. *Trends Biochem. Sci. 23*, 179−184.

(15) Fraser, C., Dawson, J. C., Dowling, R., Houston, D. R., Weiss, J. T., Munro, A. F., Muir, M., Harrington, L., Webster, S. P., Frame, M. C., Brunton, V. G., Patton, E. E., Carragher, N. O., and Unciti-Broceta, A. (2016) Rapid Discovery and Structure-Activity Relationships of Pyrazolopyrimidines That Potently Suppress Breast Cancer Cell Growth via SRC Kinase Inhibition with Exceptional Selectivity over ABL Kinase. *J. Med. Chem. 59*, 4697−4710.

(16) Brandvold, K. R., Santos, S. M., Breen, M. E., Lachacz, E. J., Steffey, M. E., and Soellner, M. B. (2015) Exquisitely specific bisubstrate inhibitors of c-Src kinase. *ACS Chem. Biol. 10*, 1387−1391.

(17) Aleem, S., Georghiou, G., Kleiner, R. E., Guja, K., Craddock, B. P., Lyczek, A., Chan, A. I., Garcia-Diaz, M., Miller, W. T., Liu, D. R., and Seeliger, M. A. (2016) Structural and Biochemical Basis for Intracellular Kinase Inhibition by Src-specific Peptidic Macrocycles. *Cell Chem. Biol. 23*, 1103−1112.

(18) Wallace, A. C., Laskowski, R. A., and Thornton, J. M. (1995) LIGPLOT: a program to generate schematic diagrams of protein-ligand interactions. *Protein Eng., Des. Sel. 8*, 127−134.

(19) Leonard, S. E., Register, A. C., Krishnamurty, R., Brighty, G. J., and Maly, D. J. (2014) Divergent modulation of Src-family kinase regulatory interactions with ATP-competitive inhibitors. *ACS Chem. Biol. 9*, 1894−1905.

(20) Register, A. C., Leonard, S. E., and Maly, D. J. (2014) SH2-catalytic domain linker heterogeneity influences allosteric coupling across the SFK family. *Biochemistry 53*, 6910−6923.

(21) Stachlewitz, R. F., Hart, M. A., Bettencourt, B., Kebede, T., Schwartz, A., Ratnofsky, S. E., Calderwood, D. J., Waegell, W. O., and Hirst, G. C. (2005) A-770041, a novel and selective small-molecule inhibitor of Lck, prevents heart allograft rejection. *J. Pharmacol. Exp. Ther. 315*, 36−41.

(22) Wang, Q., Cahill, S. M., Blumenstein, M., and Lawrence, D. S. (2006) Self-reporting fluorescent substrates of protein tyrosine kinases. *J. Am. Chem. Soc. 128*, 1808−1809.

(23) Register, A. C., Chakraborty, S., and Maly, D. J. (2017) Allosteric Modulation of Src Family Kinases with ATP-Competitive Inhibitors. *Methods Mol. Biol. 1636*, 79−89.
(24) Bantscheff, M., Eberhard, D., Abraham, Y., Bastuck, S., Boesche, M., Hobson, S., Mathieson, T., Perrin, J., Raida, M., Rau, C., Reader, V., Sweetman, G., Bauer, A., Bouwmeester, T., Hopf, C., Kruse, U., Neubauer, G., Ramsden, N., Rick, J., Kuster, B., and Drewes, G. (2007) Quantitative chemical proteomics reveals mechanisms of action of clinical ABL kinase inhibitors. *Nat. Biotechnol. 25*, 1035−1044.
(25) Golkowski, M., Brigham, J. L., Perera, G. K., Romano, G. E., Maly, D. J., and Ong, S. E. (2014) Rapid profiling of protein kinase inhibitors by quantitative proteomics. *MedChemComm 5*, 363−369.
(26) Golkowski, M., Perera, G. K., Vidadala, V. N., Ojo, K. K., Van Voorhis, W. C., Maly, D. J., and Ong, S. E. (2018) Kinome chemoproteomics characterization of pyrrolo[3,4-c]pyrazoles as potent and selective inhibitors of glycogen synthase kinase 3. *Mol. Omics 14*, 26−36.
(27) Golkowski, M., Vidadala, R. S., Lombard, C. K., Suh, H. W., Maly, D. J., and Ong, S. E. (2017) Kinobead and Single-Shot LC-MS Profiling Identifies Selective PKD Inhibitors. *J. Proteome Res. 16*, 1216−1227.
(28) Eid, S., Turk, S., Volkamer, A., Rippmann, F., and Fulle, S. (2017) KinMap: a web-based tool for interactive navigation through human kinome data. *BMC Bioinf. 18*, 16.
(29) Hari, S. B., Perera, B. G., Ranjitkar, P., Seeliger, M. A., and Maly, D. J. (2013) Conformation-selective inhibitors reveal differences in the activation and phosphate-binding loops of the tyrosine kinases Abl and Src. *ACS Chem. Biol. 8*, 2734−2743.
(30) Wodicka, L. M., Ciceri, P., Davis, M. I., Hunt, J. P., Floyd, M., Salerno, S., Hua, X. H., Ford, J. M., Armstrong, R. C., Zarrinkar, P. P., and Treiber, D. K. (2010) Activation state-dependent binding of small molecule kinase inhibitors: structural insights from biochemistry. *Chem. Biol. 17*, 1241−1249.
(31) Lombard, C. K., Davis, A. L., Inukai, T., and Maly, D. J. (2018) Allosteric Modulation of JNK Docking Site Interactions with ATP-Competitive Inhibitors. *Biochemistry 57*, 5897−5909.
(32) Krishnamurty, R., Brigham, J. L., Leonard, S. E., Ranjitkar, P., Larson, E. T., Dale, E. J., Merritt, E. A., and Maly, D. J. (2013) Active site profiling reveals coupling between domains in SRC-family kinases. *Nat. Chem. Biol. 9*, 43−50.
(33) Young, M. A., Gonfloni, S., Superti-Furga, G., Roux, B., and Kuriyan, J. (2001) Dynamic coupling between the SH2 and SH3 domains of c-Src and Hck underlies their inactivation by C-terminal tyrosine phosphorylation. *Cell 105*, 115−126.
(34) Theile, C. S., Witte, M. D., Blom, A. E., Kundrat, L., Ploegh, H. L., and Guimaraes, C. P. (2013) Site-specific N-terminal labeling of proteins using sortase-mediated reactions. *Nat. Protoc. 8*, 1800−1807.
(35) Ayrapetov, M. K., Wang, Y. H., Lin, X., Gu, X., Parang, K., and Sun, G. (2006) Conformational basis for SH2-Tyr(P)527 binding in Src inactivation. *J. Biol. Chem. 281*, 23776−23784.
(36) Okada, M., Nada, S., Yamanashi, Y., Yamamoto, T., and Nakagawa, H. (1991) CSK: a protein-tyrosine kinase involved in regulation of src family kinases. *J. Biol. Chem. 266*, 24249−24252.
(37) Levinson, N. M., Seeliger, M. A., Cole, P. A., and Kuriyan, J. (2008) Structural basis for the recognition of c-Src by its inactivator Csk. *Cell 134*, 124−134.
(38) Okada, M. (2012) Regulation of the SRC family kinases by Csk. *Int. J. Biol. Sci. 8*, 1385−1397.
(39) Staben, S. T., Feng, J. A., Lyle, K., Belvin, M., Boggs, J., Burch, J. D., Chua, C. C., Cui, H., DiPasquale, A. G., Friedman, L. S., Heise, C., Koeppen, H., Kotey, A., Mintzer, R., Oh, A., Roberts, D. A., Rouge, L., Rudolph, J., Tam, C., Wang, W., Xiao, Y., Young, A., Zhang, Y., and Hoeflich, K. P. (2014) Back pocket flexibility provides group II p21-activated kinase (PAK) selectivity for type I 1/2 kinase inhibitors. *J. Med. Chem. 57*, 1033−1045.

DOI: 10.1021/acschembio.9b00214
ACS Chem. Biol. 2019, 14, 1249−1259